

RESEARCH REPORT

ALTERED MERISTEM PROGRAM1 regulates leaf identity independently of miR156-mediated translational repression

Jim P. Fouracre, Victoria J. Chen and R. Scott Poethig*

ABSTRACT

In *Arabidopsis*, loss of the carboxypeptidase ALTERED MERISTEM PROGRAM1 (AMP1) produces an increase in the rate of leaf initiation, an enlarged shoot apical meristem and an increase in the number of juvenile leaves. This phenotype is also observed in plants with reduced levels of miR156-targeted *SQUAMOSA PROMOTER BINDING PROTEIN-LIKE* (*SPL*) transcription factors, suggesting that AMP1 might promote *SPL* activity. However, we found that the *amp1* mutant phenotype is only partially corrected by elevated *SPL* gene expression, and that *amp1* has no significant effect on *SPL* transcript levels, or on the level or the activity of miR156. Although AMP1 has been reported to promote miRNA-mediated translational repression, *amp1* did not prevent the translational repression of the miR156 target *SPL9* or the miR159 target *MYB33*. These results suggest that AMP1 regulates vegetative phase change downstream of, or in parallel to, the miR156/*SPL* pathway, and that it is not universally required for miRNA-mediated translational repression.

KEY WORDS: Vegetative phase change, AMP1, miR156, SPL, Translational repression, miR159

INTRODUCTION

Plant life histories are underpinned by a series of developmental transitions, the correct timing of which are crucial for plant survival and reproductive success (Huijser and Schmid, 2011). Early in their development, plants transition from a juvenile to an adult phase of vegetative growth (vegetative phase change, VPC). This transition is regulated by a decline in the abundance of two miRNAs, miR156 and miR157, which results in an increase in the expression of their targets, *SQUAMOSA PROMOTER BINDING PROTEIN-LIKE* (*SPL*) transcription factors. These transcription factors promote the expression of adult vegetative traits, in part by promoting the expression of miR172 (Wu and Poethig, 2006; Wu et al., 2009). VPC is thus regulated by inverse gradients of expression of two miRNAs, miR156 and miR172.

ALTERED MERISTEM PROGRAM1 (*AMP1*) encodes a putative carboxypeptidase (Helliwell et al., 2001), and was identified in a genetic screen for juvenilized mutants over 20 years ago (Conway and Poethig, 1997). Mutations in *AMP1* produce a large number of small round leaves that lack abaxial trichomes (juvenile leaves) and have a higher rate of leaf initiation (Telfer et al., 1997). An initial study suggested that this phenotype was not associated with a

change in the timing of VPC, implying that the timing of VPC is regulated independently of leaf number (Telfer et al., 1997). However, this result conflicts with more recent studies showing that pre-existing leaves promote VPC (Yang et al., 2011, 2013; Yu et al., 2013). The phenotype of *amp1* is also surprising given the evidence that AMP1 is required for miRNA-mediated translational repression (Li et al., 2013). miR156 regulates the expression of its targets primarily by promoting their translational repression (He et al., 2018). Consequently, *amp1* mutants are expected to have a reduced number of juvenile leaves due to elevated *SPL* gene expression, which is the exact opposite of the *amp1* phenotype.

To resolve these issues, we investigated the interaction between *AMP1* and the miR156-*SPL* module. Our results indicate that *AMP1* promotes adult leaf traits in parallel to, or downstream of, the miR156-*SPL* module. We also found no evidence that AMP1 is required for translational repression by either miR156 or miR159. This latter result suggests that the mechanism by which miRNAs repress translation in plants is different for different transcripts.


RESULTS AND DISCUSSION

Elevated *SPL* activity has a modest effect on the *amp1* phenotype

amp1-1 (hereafter, *amp1*) mutants resemble plants with reduced *SPL* gene expression in having an increased rate of leaf initiation, an increased number of rosette leaves, an enlarged shoot apical meristem (SAM), and small, round rosette leaves that lack abaxial trichomes (Fig. 1A-F) (Chaudhury et al., 1993; Huang et al., 2015; Telfer et al., 1997; Yang et al., 2018). To determine whether this phenotype is attributable to a reduction in *SPL* activity, we constitutively expressed the miR156 target site mimic *MIM156* in *amp1*. *MIM156* sequesters endogenous miR156 and leads to a de-repression of *SPL* gene activity (Franco-Zorrilla et al., 2007). *35S::MIM156* plants have a relatively slow rate of leaf initiation, have enlarged and somewhat elongated rosette leaves, produce abaxial trichomes unusually early in shoot development, and have a relatively small SAM (Fig. 1A-F). *amp1; 35S::MIM156* plants had a vegetative phenotype intermediate between that of the two parental genotypes but which was more similar to *amp1* than to *35S::MIM156*. The rosette leaves of *amp1; 35S::MIM156* were approximately the same size as *amp1* leaves but were similar in shape to *35S::MIM156* (Fig. 1A,B). *amp1* plants rarely produced rosette leaves with abaxial trichomes (although abaxial trichome production on cauline leaves was unaffected; Fig. S1), whereas about 25% of *amp1; 35S::MIM156* produced rosette leaves with abaxial trichomes late in shoot development. In contrast, all *35S::MIM156* plants produced rosette leaves with abaxial trichomes by plastochron 3 (Fig. 1C). Similarly, the rate of leaf initiation (Fig. 1D) and total rosette leaf number (Fig. 1E) in *amp1; 35S::MIM156* were closer to that of *amp1* than *35S::MIM156*. Finally, the SAM of *amp1; 35S::MIM156* was more similar in size to *amp1* than to *35S::MIM156* (Fig. 1F). To confirm that the *amp1* phenotype does not

Biology Department, University of Pennsylvania, 433 S. University Ave, Philadelphia, PA 19104, USA.

*Author for correspondence (spoethig@sas.upenn.edu)

 J.P.F., 0000-0003-0049-3047; R.S.P., 0000-0001-6592-5862

Handling Editor: Ykä Helariutta
Received 27 November 2019; Accepted 5 March 2020

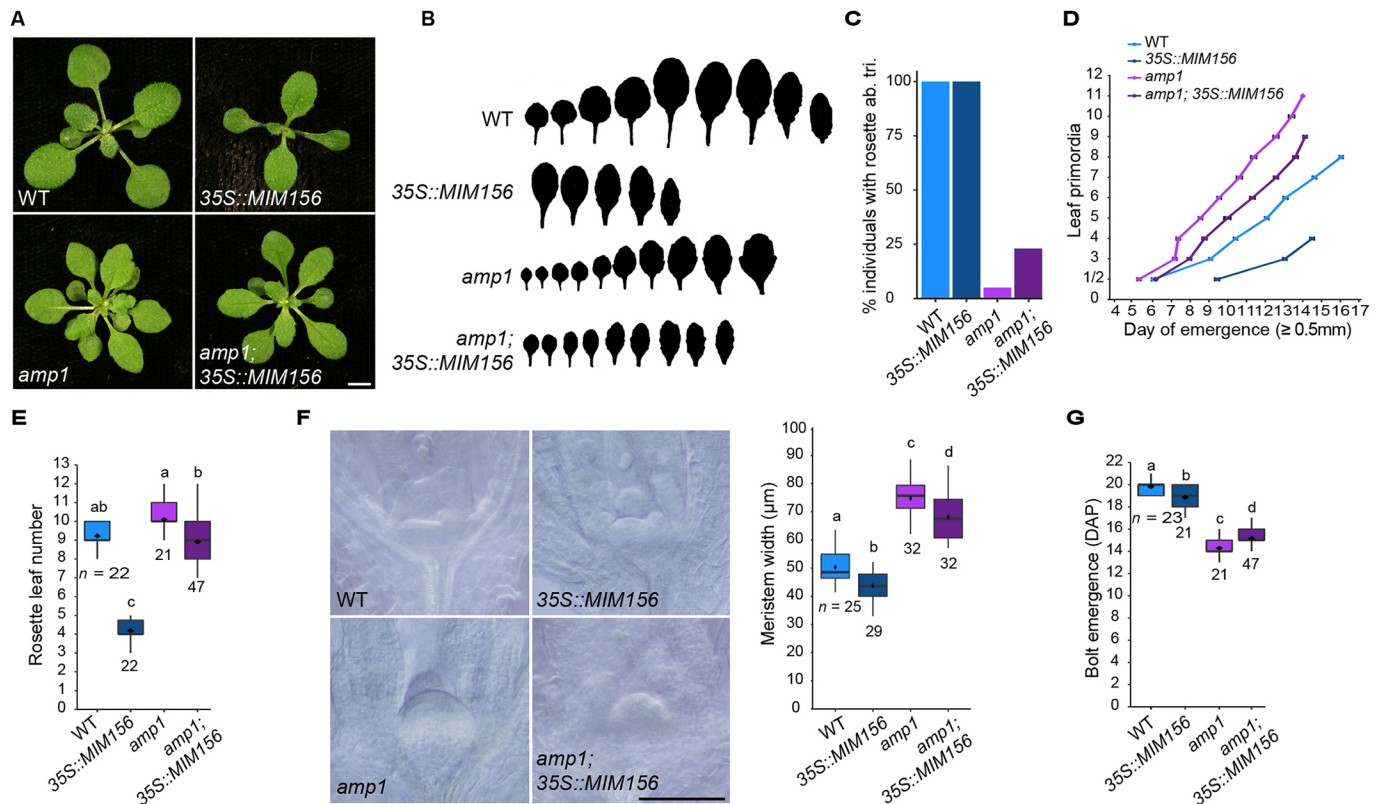


Fig. 1. Elevated *SPL* gene activity only partially suppresses the *amp1* phenotype. (A) Plants at 16 DAG. (B) Silhouettes of rosette leaves for the lines shown in A. (C) Percentage of individual plants that produced at least one rosette leaf with abaxial trichomes (ab. tri.) ($n \geq 18$). (D) Leaf primordia emergence was scored when leaves became visible without manipulation of the rosette. Data represent the mean \pm s.e.m ($n \geq 18$). (E) Total number of rosette leaves. (F) SAM size at 5 DAG. Images were taken using DIC microscopy, measurements were taken at the widest point of the SAM between emerging leaf primordia. (G) Inflorescence bolts were scored the day they visibly protruded from the rosette. Statistically distinct genotypes were identified by one-way ANOVA with post-hoc Tukey's multiple comparison test (letters indicate statistically distinct groups; $P < 0.05$). All phenotypic analyses were carried out in LD. WT, wild type. Scale bars: 5 mm (A); 100 μ m (F).

require miR156, we expressed a miR156-resistant version of *SPL9* (*rSPL9*) in *amp1*. The phenotypes of *amp1*; *rSPL9* and *amp1*; *35S::MIM156* plants were highly similar (Fig. S2). Taken together, these results suggest that the phenotype of *amp1* is not a consequence of miR156-mediated repression of *SPL* activity, implying that *AMP1* acts either downstream of, or in parallel to, the miR156-*SPL* module. This conclusion is consistent with the observation that *amp1* plants flower earlier than wild type (Fig. 1G) despite remaining in the juvenile phase (Fig. 1C).

The phenotype of *amp1* is not attributable to a change in miR156/miR157 or *SPL* gene expression

To explore the relationship between *AMP1* and the miR156-*SPL* module in more detail, we examined the effect of *amp1* on the abundance of miR156 and *SPL* transcripts. qRT-PCR analysis of the shoot apices of plants grown in short days (SD) showed that *amp1* had no consistent effect on the level of miR156 or miR157 (Fig. 2A), or the transcripts of three direct targets of these miRNAs: *SPL3*, *SPL9* and *SPL13* (Fig. 2B). To test whether *amp1* affects *SPL* expression independent of miR156 and miR157, we measured the transcripts of these genes in *35S::MIM156* and *amp1*; *35S::MIM156* plants. As expected (He et al., 2018), all three *SPL* transcripts were significantly elevated in *35S::MIM156* relative to wild type. All three transcripts were elevated to a much lesser extent in *amp1*; *35S::MIM156* than *35S::MIM156* (Fig. 2B). Together, these results suggest that *AMP1* may transcriptionally regulate *SPL*

expression, but only in the absence of miR156/miR157. The reduced accumulation of *SPL* transcripts in *amp1*; *35S::MIM156* relative to *35S::MIM156* plants could also be explained either by silencing of the *MIM156* transgene, or by suppression of miR156 sequestration by *MIM156* in the *amp1* background. However, we found no evidence that *MIM156* is silenced in *amp1* (Fig. S2G), and the similarity between the *amp1*; *35S::MIM156* and *amp1*; *rSPL9* phenotypes (Fig. S2A-F) suggests that miR156-sequestration is functional in *amp1*; *35S::MIM156*.

We then examined the expression of these genes in successive rosette leaf primordia (LP) of plants grown in SD. Because *amp1* initiates leaves more rapidly than wild type, LP were grouped according to the time of harvest rather than position on the shoot. Both the level and rate of decline of miR156 were almost identical in wild type and *amp1* (Fig. 2C). miR157 was elevated in all LP, but declined at approximately the same rate as in wild-type plants. *SPL9* and *SPL13* transcripts were also elevated in the LP of *amp1* relative to wild type (Fig. 2D), but these differences were relatively modest (twofold or less) and not statistically significant. Taken together, these data suggest that the vegetative phenotype of *amp1* is not caused by increased expression of miR156/miR157 or decreased expression of *SPL* genes. It is possible that *AMP1* regulates *SPL* expression independently of miR156 (Fig. 2B). However, the observation that *amp1* does not have a significant effect on *SPL9* and *SPL13* expression at 20 days after germination (DAG) (Fig. 2D), when the levels of miR156 and miR157 are very low (Fig. 2C), suggests that this is unlikely.

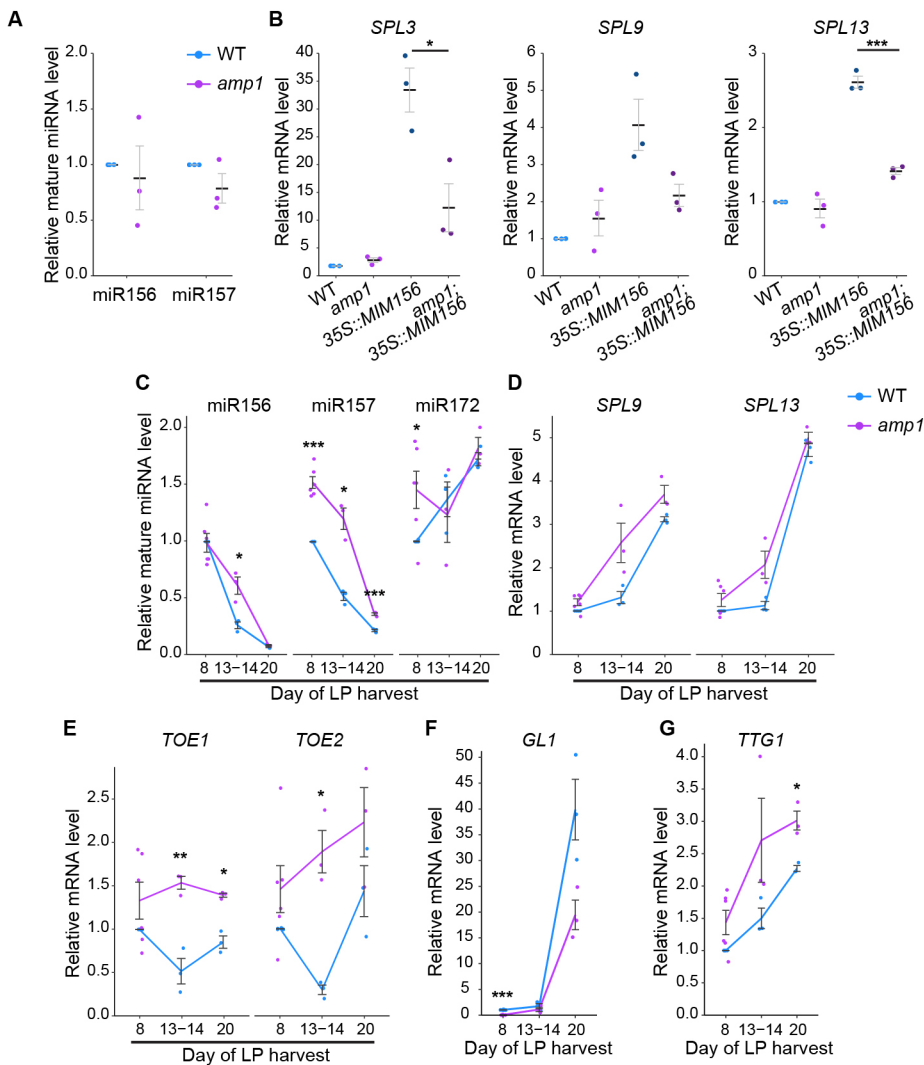


Fig. 2. The *amp1* phenotype is not associated with repressed SPL activity. (A-G) qRT-PCR analyses of gene expression. (A,B) Shoot apices with LP ≥ 1 mm removed at 8 DAG. (C-G) Isolated LP 0.5-1 mm in size. 8 DAG=LP1-2; 13-14 DAG=LP 4-5 [*amp1* LP were harvested at 13 DAG and wild-type (WT) LP at 14 DAG]; 20 DAG=wild-type LP9-10, *amp1* LP14-16. Data represent the mean \pm s.e.m. All plants were grown in SD conditions. Asterisks represent significant differences between genotypes calculated by an unpaired two-tailed Student's *t*-test (* $P < 0.05$; ** $P < 0.01$; *** $P < 0.001$).

To determine whether AMP1 regulates the expression of genes downstream of the miR156-SPL module, we examined the expression of two *AP2*-like transcription factors, *TOE1* and *TOE2*, which are targets of the SPL-regulated miRNA miR172. The transcripts of both genes were generally elevated in *amp1* (Fig. 2E), and this effect was not attributable to a change in the level of miR172 because *amp1* had no effect on this miRNA (Fig. 2C). *TOE1* inhibits trichome production on the abaxial side of the leaf by repressing the transcription of *GLABRA1* (*GL1*) in association with the abaxial specification gene, *KANADI* (*KANI*) (Wang et al., 2019; Xu et al., 2019). In wild-type plants, *GL1* expression increased dramatically at 13-14 DAG and 20 DAG, consistent with the increase in abaxial trichome production over this period. *GL1* had a similar temporal pattern in *amp1* but was almost completely absent in the earliest LP, and was present at much lower levels than wild type in LP harvested at 20 DAG (Fig. 2F). In contrast, the expression of *TRANSPARENT TESTA GLABRA1* (*TTG1*), which promotes trichome initiation in parallel to *GL1* (Pesch et al., 2015), was actually elevated in *amp1* (Fig. 2G). These results suggest that *AMP1* promotes abaxial trichome formation via *GL1*, not *TTG1*, and that it acts downstream of miR156-SPL. However, whether the effect of *amp1* on trichome production depends on *TOE1* remains to be determined.

The timing of vegetative phase change is regulated independently of leaf initiation in *amp1*

The juvenilized phenotype of *amp1* was originally attributed to the increased rate of leaf initiation in this mutant (Telfer et al., 1997). However, this interpretation is inconsistent with more recent studies showing that pre-existing leaves promote the transition to the adult vegetative phase by repressing miR156 (Yang et al., 2011, 2013; Yu et al., 2013). To determine the basis of this discrepancy, we characterized the effect of *CLAVATA3* (*CLV3*) and *CLV1* mutations on VPC. We chose these mutations because they resemble *amp1* in having an enlarged SAM and an accelerated rate of leaf initiation (Clark et al., 1995; Leyser and Furger, 1992).

Like *amp1* (Telfer et al., 1997), *clv3* and *clv1* produced smaller rounder rosette leaves, and more leaves without abaxial trichomes (Fig. 3A-C). However, this increase in the number of juvenile-like leaves was not associated with a delay in the juvenile-to-adult transition. Instead, *clv3* mutants produced leaves with abaxial trichomes 1 day earlier than wild-type plants (Fig. 3D). To determine whether the phenotype of *clv1* and *clv3* is dependent on miR156, we introduced *35S::MIM156* into these mutants. This transgene was epistatic to *clv1* and *clv3* with respect to their effect on leaf shape (Fig. 3A,B) and abaxial trichome production (Fig. 3C), suggesting that their effect on these traits requires miR156.

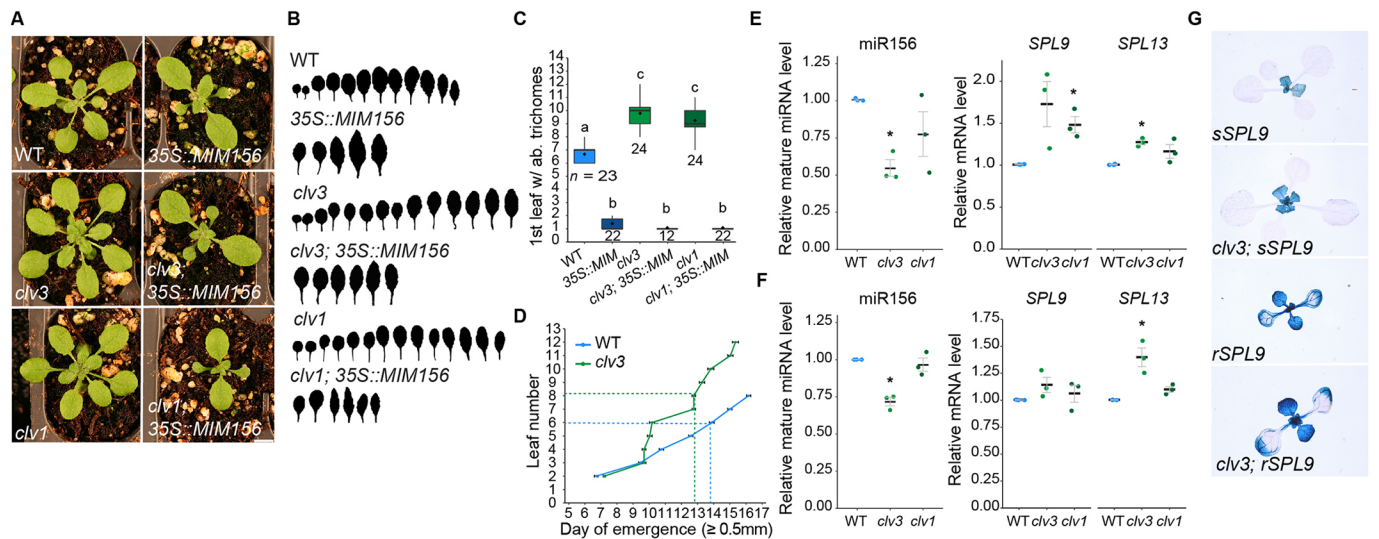


Fig. 3. Enhanced *clv* juvenility is a consequence of an increased rate of leaf initiation, rather than repressed *SPL* gene activity. (A) Plants at 21 DAG. Scale bar: 5 mm. (B) Silhouettes of rosette leaves for the lines shown in A. (C) First leaf to produce abaxial trichomes. Statistically distinct genotypes were identified by one-way ANOVA with post-hoc Tukey's multiple comparison test (letters indicate statistically distinct groups; $P < 0.05$). (D) Leaf emergence was scored when leaves became visible without manipulation of the rosette. The dashed lines indicate the first leaf to produce abaxial trichomes. Data represent the mean \pm s.e.m. ($n \geq 23$). (E, F) qRT-PCR analyses of gene expression of (E) shoot apices with leaf primordia ≥ 1 mm removed at 10 DAG and (F) isolated LP1 and LP2 0.5–1 mm in size. Asterisks represent significant differences between wild type (WT) versus *clv3* or WT versus *clv1*. Significance was calculated by an unpaired two-tailed Student's *t*-test ($P < 0.05$). (G) Staining of miR156-sensitive and miR156-resistant *SPL*-GUS reporter constructs at 14 DAG. Phenotypic analyses were carried out in LD (A–D) and gene expression analyses were carried out in SD (E–G).

We then examined the effect of *clv3* and *clv1* on the expression of miR156 and its targets, *SPL9* and *SPL13*, in shoot apices (Fig. 3E) and LP (Fig. 3F). qRT-PCR revealed that *clv1* and *clv3* have slightly reduced levels of miR156, and elevated levels of *SPL9* and *SPL13*, although these differences were only statistically significant in a few cases. If these relatively small differences in miR156 and *SPL* gene expression are functionally significant, they would be expected to promote the appearance of adult traits, not repress the expression of these traits as is the case in *clv1* and *clv3*. To explore this inconsistency, we examined the effect of *clv3* on the expression of miR156-sensitive (*sSPL9*) and miR156-resistant (*rSPL9*) versions of the *SPL9::SPL9-GUS* reporter (Xu et al., 2016). There was no obvious difference in the expression of these reporters in the presence or absence of *clv3* (Fig. 3G), supporting the conclusion that the effect of *clv3* on leaf identity is not attributable to a change in the level of miR156 or its targets.

Instead, the effect of *clv3* and *clv1* on leaf identity is primarily attributable to their effect on the rate of leaf initiation. Specifically, *clv3* and *clv1* appear to increase the number of juvenile leaves by accelerating the rate of leaf production during the period when miR156 levels are high. This conclusion is supported by the observation that *35S::MIM156* is epistatic to these mutations with respect to their effect on leaf identity (Fig. 3A,B), i.e. miR156 is required for their leaf identity phenotypes. Consistent with the evidence that leaves promote the juvenile-to-adult transition by repressing miR156 (Yang et al., 2011, 2013; Yu et al., 2013), *clv3* and *clv1* have slightly reduced levels of miR156 and slightly elevated levels of *SPL9* and *SPL13* (Fig. 3E,F). However, this relatively small effect is apparently insufficient to interfere with the function of these genes in specifying juvenile leaf identity.

The increased number of juvenile leaves in *amp1* is also partly attributable to its higher rate of leaf initiation (Telfer et al., 1997). However, *amp1* differs from *clv3* and *clv1* in having a much more significant effect on leaf identity. In addition, the phenotype of *amp1* is less sensitive to a reduction in miR156 than the phenotype of *clv3* and *clv1* (Fig. 1A–E; Fig. 2A–D). This observation, and the effect of *amp1*

on the expression of genes involved in abaxial trichome production (Fig. 2E,F), suggest that AMP1 operates independently of miR156 to regulate genes involved in leaf identity. A direct effect of AMP1 on leaf identity genes would explain why *amp1* has a more severe vegetative phenotype than *clv3* and *clv1*, and why the phenotype of *amp1* is relatively insensitive to changes in the level of miR156.

AMP1 is not universally required for translational repression

Given the role of *AMP1* in translational repression (Li et al., 2013), it is possible that the abundance of *SPL* transcripts in *amp1* (Fig. 2B,D) does not accurately reflect their biological activity. To determine whether AMP1 is required for the post-translational regulation of *SPL* genes, we first measured the amount of *SPL9* and *SPL13* transcript cleavage in wild-type and *amp1* plants. Consistent with a previous study on miR156-mediated cleavage (He et al., 2018), the rate of transcript cleavage for both *SPL9* and *SPL13* declined during vegetative development in wild-type plants (Fig. 4A). For *SPL9*, this happened at a slower rate in *amp1*, presumably in part because of the higher level of miR156 in the *amp1* 13–14 DAG sample compared with wild type (Fig. 2C), and the threshold-dependence of miR156 activity (He et al., 2018). However, later in development, transcript cleavage for both *SPL9* and *SPL13* in *amp1* was similar to wild type (Fig. 4A). This demonstrates that miR156 is functional in *amp1* and confirms the observation that AMP1 is not required for transcriptional cleavage (Li et al., 2013).

Although miR156 induces transcript cleavage, it represses the expression of its targets primarily by promoting translational repression (He et al., 2018). To examine the effect of *amp1* on this process, we crossed *sSPL9* and *rSPL9* GUS-reporter constructs into *amp1*. There was no obvious difference in the staining intensity of these reporter proteins in wild type and *amp1* (Fig. 4B). This impression was confirmed by spectrophotometric intensity measurements of the *sSPL9*-GUS reporter in LP of wild type and *amp1* harvested at 20 DAG (Fig. 4C,D), a time point at which transcript cleavage was nearly equivalent in these genotypes

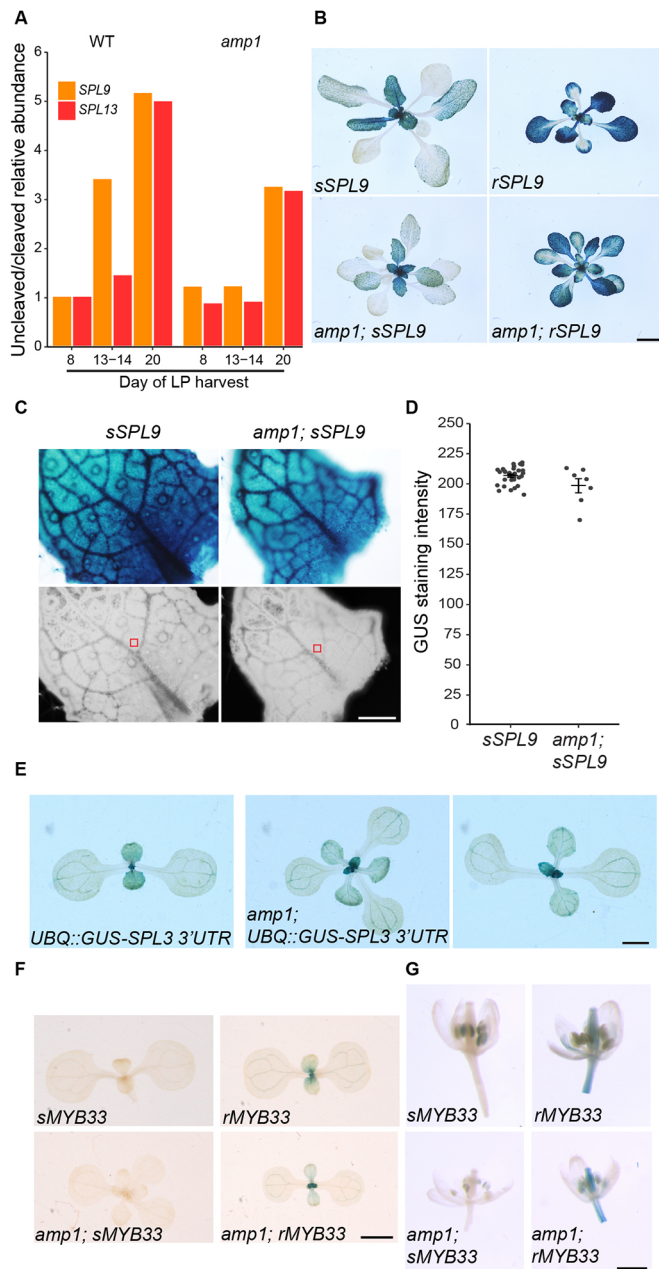


Fig. 4. miRNA-regulated SPL9 and MYB33 proteins accumulate normally in *amp1*. (A) The relative abundance of uncleaved/cleaved transcripts, normalized to wild type (WT) 8 DAG. See Fig. 2 legend for details of samples. (B) Staining of miR156-sensitive and miR156-resistant SPL-GUS reporter constructs at 21 DAG. (C,D) Quantification of sSPL9-GUS protein levels by image analysis. In C, top panels show RGB color mode and bottom panels hue saturation brightness mode. Red squares indicate where signal intensity was measured. In D, each dot represents an individual primordia. Data represent the mean \pm s.e.m. (E-G) Staining of GUS reporter constructs in 8 DAG seedlings (staining in two phenotypically distinct *amp1* individuals is shown) (E), 7 DAG seedlings (F) and flowers (G). Scale bars: 5 mm (B); 200 μ m (C); 1 mm (E-G).

(Fig. 4A). These results indicate that *amp1* has no effect on the repression of *SPL9* by miR156. To test whether translational repression in *amp1* is affected in other *SPL*-sequence and expression contexts, we introduced a miR156-sensitive *UBIQUITIN10::GUS-SPL3 3'UTR* reporter construct into wild-type and *amp1* backgrounds (Fig. 4E). There was no obvious difference in the expression of this reporter in these genotypes, providing further

support for the conclusion that *AMP1* is not required for miR156 activity.

To determine whether miR156 is uniquely insensitive to *amp1*, we examined the effect of *amp1* on the expression of *MYB33*, a transcription factor that also regulates shoot identity (Guo et al., 2017) and is translationally repressed by miR159 (Li et al., 2014). miR159-sensitive and miR159-resistant versions of *MYB33-GUS* (Millar and Gubler, 2005) were crossed into *amp1*, and wild-type and *amp1* plants were stained for GUS activity 1 week after germination, and at flowering. *MYB33-GUS* was repressed in a miR159-dependent fashion in leaves and floral organs of wild-type plants, and *amp1* had no obvious effect on this expression pattern (Fig. 4F,G). We conclude from these results that *AMP1* is not universally required for the translational repression of miRNA-targets.

Whether or not *AMP1* functions in translational repression might depend on the subcellular localization of this process. *AMP1* has been shown to colocalize with the key silencing component ARGONAUTE1 (AGO1) on the endoplasmic reticulum (ER) (Li et al., 2013). However, AGO1 also localizes to processing bodies (p-bodies), which are cytoplasmic mRNA-ribonucleoprotein complexes involved in translational silencing (reviewed by Chantarachot and Bailey-Serres, 2018). Loss of the p-body protein SUO leads to a reduction in the translational repression of the miR156-target *SPL3* (Yang et al., 2012), suggesting that p-bodies are also important sites of miRNA-mediated translational repression. These results suggest that miRNA-mediated translational repression occurs in distinct subcellular compartments in a sequence-specific manner, and that unique sets of proteins function in each compartment (e.g. *AMP1* on the ER, SUO in p-bodies). This model is supported by the observation that isoprenoid biosynthesis, which is necessary for the formation of membrane-bound compartments, is required for miRNA activity (Brodersen et al., 2012).

How different miRNA-mRNA complexes are targeted to different cytoplasmic compartments is unclear. *AMP1*-dependent miRNAs appear to have an increased number of bulges in the precursor hairpin relative to *AMP1*-independent miRNAs (Fig. S3), although it is perhaps unlikely that any such signals would persist during miRNA processing. The strength of target complementarity is known to affect silencing efficacy (Li et al., 2014), and could also drive subcellular distribution, but there is also no trend in target mismatch number between the *AMP1*-dependent/independent classes of miRNA (Table S1). Given the overlapping expression domains of a number of these miRNAs and *AMP1* (Fouracre and Poethig, 2016; Vidaurre et al., 2007), it is unlikely that the site of translational repression is either developmentally regulated or determined by *AMP1* localization. At the cellular level, there is evidence to suggest that miRNA sequences include signals that control the specificity of intercellular mobility (Skopelitis et al., 2018). It will be fascinating to see if the same signaling mechanisms determine the destination of miRNAs within cells.

MATERIALS AND METHODS

Plant material and growth conditions

All stocks were in a Col-0 background. The following genetic lines have been described previously: *amp1-1* (Chaudhury et al., 1993); *SPL9::sSPL9-GUS*, *SPL9::rSPL9-GUS* (Xu et al., 2016); *35S::MIM156* (Fouracre and Poethig, 2019); *chl-4* (Clark et al., 1993); and *MYB33::sMYB33-GUS*, *MYB33::rMYB33-GUS* (Millar and Gubler, 2005). *chl3-10* (CS68823) was obtained from the Arabidopsis Biological Resource Center (Ohio State University, OH, USA). Seeds were sown on fertilized Farfard #2 soil (Farfard) and kept at 4°C for 3 days prior to transfer to a growth chamber, with the transfer day counted as day 0 for plant age (0 DAG). Plants were

grown at 22°C under a mix of both white (USHIO F32T8/741) and red-enriched (Interlectric F32/T8/WS Gro Lite) fluorescent bulbs in either long day (LD; 16 h light/8 h dark; 80 $\mu\text{mol m}^{-2} \text{s}^{-1}$) or SD (10 h light/14 h dark; 120 $\mu\text{mol m}^{-2} \text{s}^{-1}$) conditions.

Generation of *UBIQUITIN::GUS-SPL3' 3'UTR* reporter line

A 650 bp fragment of the *UBIQUITIN10* (At4g05320) promoter and a 400 bp fragment downstream of the *SPL3* (At2g33810) stop codon (which contains a miR156 target site) were cloned from *Arabidopsis* genomic DNA and adapted to the Golden Gate cloning system (Engler et al., 2014). These were combined with the β -glucuronidase sequence from *Escherichia coli* (pICH7511) to generate a *UBQ10::GUS-SPL3 3'UTR* transcriptional unit in the pAGM4723 binary vector, using the pFAST-R selection cassette as a selectable marker. Cloning and binary vectors were part of the MoClo cloning toolbox provided by Addgene. Cloning primer sequences are provided in Table S2.

GUS staining

Plants were fixed in 90% acetone on ice for 10 min and washed with GUS staining buffer (5 mM potassium ferricyanide and 5 mM ferrocyanide in 0.1 M PO_4 buffer) and stained for between 8 h and overnight (depending on transgene strength) at 37°C in 2 mM X-Gluc GUS staining buffer. For the quantification of GUS staining intensity, ~1 mm LP were harvested at 21 DAG, stained overnight and images of stained primordia converted from RGB color mode to hue saturation brightness mode as described previously (Béziat et al., 2017). A consistent position in the middle of the leaf lamina, adjacent to the midvein, was used for measurement.

Histology

Shoot apices were cleared and imaged using DIC microscopy according to a protocol described previously (Chou et al., 2016).

RNA expression analyses

Tissue [either shoot apices with leaf primordia (≤ 1 mm attached), or isolated leaf primordia (0.5–1 mm in size) – sample type is detailed in the respective figure legend] were ground in liquid nitrogen and total RNA extracted using Trizol (Invitrogen) as per the manufacturer's instructions. RNA was DNase treated with RQ1 (Promega) and 250 ng-1 μg of RNA was used for reverse transcription using Superscript III Reverse Transcriptase (Invitrogen). Gene-specific reverse transcription primers were used to amplify miR156, miR157, miR172 and SnoR101, and a polyT primer was used for mRNA amplification. Three-step qPCR of cDNA was carried out using SYBR-Green Master Mix (Bimake). qPCR reactions were run in triplicate and an average was calculated. For analyses of *amp1* shoot apices and *clv* mutants, separate RNA extractions of three biological replicates were carried out. For analyses of *amp1* leaf primordia, three reverse-transcription replicates from single RNA extractions were carried out for each sample (at least 60 LP were pooled for each RNA extraction). Two biological replicates were harvested at 8 DAG – once as part of a biological replicate with 13–14 DAG samples, and once as part of a biological replicate with 20 DAG samples. Transcript levels were normalized to snoR101 (for miRNAs) and *ACT2* (*amp1* shoot apices, *clv* mutants), or *UBQ10* (*amp1* leaf primordia) (for mRNAs), and expressed relative to wild type (*amp1* shoot apices, *clv* mutants) and wild-type 8 DAG (*amp1* leaf primordia) samples.

For the quantification of transcript cleavage, a modified 5'RACE protocol was followed as described previously (He et al., 2018). The data presented are the average of three ratios from separate reverse transcription replicates (six in the case of *amp1* 8 DAG – three reverse transcription replicates from two biological replicates). The qPCR primers used in this study are listed in Table S2.

Statistical analyses

For statistical comparisons between two genotypes, unpaired two-tailed Student's *t*-tests were carried out. For comparison of multiple samples, to decrease the chance of false positives, a one-way ANOVA, followed by a Tukey's test, was used for multi-way comparisons. Statistical analyses were carried out in R (r-project.org) and Excel (Microsoft).

For figures featuring boxplots, boxes display the interquartile range (IQR) (boxes), median (lines), and values beyond 1.5×IQR (whiskers); mean values are marked by a solid diamond.

Acknowledgements

We thank Anthony Millar (Australian National University, Australia) for the kind gift of the MYB33-GUS reporters; members of the Poethig lab for useful discussions; Xiang Yu for comments on miRNA secondary structures; and Melissa Morrison for assistance with collecting phenotypic data.

Competing interests

The authors declare no competing or financial interests.

Author contributions

Conceptualization: J.P.F., R.S.P.; Methodology: J.P.F., R.S.P.; Formal analysis: J.P.F.; Investigation: J.P.F., V.J.C.; Resources: J.P.F.; Writing - original draft: J.P.F.; Writing - review & editing: J.P.F., R.S.P.; Visualization: J.P.F.; Supervision: R.S.P.; Project administration: R.S.P.; Funding acquisition: R.S.P.

Funding

This work was supported by the National Institutes of Health (R01-GM51893 to R.S.P.). Deposited in PMC for release after 12 months.

Supplementary information

Supplementary information available online at <http://dev.biologists.org/lookup/doi/10.1242/dev.186874.supplemental>

Peer review history

The peer review history is available online at <https://dev.biologists.org/lookup/doi/10.1242/dev.186874.reviewer-comments.pdf>

References

- Béziat, C., Kleine-Vehn, J. and Feraru, E. (2017). Histochemical staining of β -glucuronidase and its spatial quantification. In *Plant Hormones: Methods and Protocols* (ed. J. Kleine-Vehn and M. Sauer), pp. 73–80. New York, NY: Springer New York.
- Brodersen, P., Sakvarelidze-Achard, L., Schaller, H., Khaff, M., Schott, G., Bendahmane, A. and Voinnet, O. (2012). Isoprenoid biosynthesis is required for miRNA function and affects membrane association of ARGONAUTE 1 in *Arabidopsis*. *Proc. Natl. Acad. Sci. USA* **109**, 1778. doi:10.1073/pnas.1112500109
- Chantarachot, T. and Bailey-Serres, J. (2018). Polysomes, stress granules, and processing bodies: a dynamic triumvirate controlling cytoplasmic mRNA fate and function. *Plant Physiol.* **176**, 254–269. doi:10.1104/pp.17.01468
- Chaudhury, A. M., Letham, S., Craig, S. and Dennis, E. S. (1993). *amp1* - a mutant with high cytokinin levels and altered embryonic pattern, faster vegetative growth, constitutive photomorphogenesis and precocious flowering. *Plant J.* **4**, 907–916. doi:10.1046/j.1365-3113.1993.04060907.x
- Chou, H., Wang, H. and Berkowitz, G. A. (2016). Shoot apical meristem size measurement. *Bio-protocol* **6**, e2055. doi:10.21769/BioProtoc.2055
- Clark, S. E., Running, M. P. and Meyerowitz, E. M. (1993). *CLAVATA1*, a regulator of meristem and flower development in *Arabidopsis*. *Development* **119**, 397–418.
- Clark, S. E., Running, M. P. and Meyerowitz, E. M. (1995). *CLAVATA3* is a specific regulator of shoot and floral meristem development affecting the same processes as *CLAVATA1*. *Development* **121**, 2057–2067.
- Conway, L. J. and Poethig, R. S. (1997). Mutations of *Arabidopsis thaliana* that transform leaves into cotyledons. *Proc. Natl. Acad. Sci. USA* **94**, 10209–10214. doi:10.1073/pnas.94.19.10209
- Engler, C., Youles, M., Gruetzner, R., Ehnert, T.-M., Werner, S., Jones, J. D. G., Patron, N. J. and Marillonnet, S. (2014). A golden gate modular cloning toolbox for plants. *ACS Synth. Biol.* **3**, 839–843. doi:10.1021/sb4001504
- Fouracre, J. P. and Poethig, R. S. (2016). The role of small RNAs in vegetative shoot development. *Curr. Opin. Plant Biol.* **29**, 64–72. doi:10.1016/j.pbi.2015.11.006
- Fouracre, J. P. and Poethig, R. S. (2019). Role for the shoot apical meristem in the specification of juvenile leaf identity in *Arabidopsis*. *Proc. Natl. Acad. Sci. USA* **116**, 10168. doi:10.1073/pnas.1817853116
- Franco-Zorrilla, J. M., Valli, A., Todesco, M., Mateos, I., Puga, M. I., Rubio-Somoza, I., Leyva, A., Weigel, D., García, J. A. and Paz-Ares, J. (2007). Target mimicry provides a new mechanism for regulation of microRNA activity. *Nat. Genet.* **39**, 1033–1037. doi:10.1038/ng2079
- Guo, C., Xu, Y., Shi, M., Lai, Y., Wu, X., Wang, H., Zhu, Z., Poethig, R. S. and Wu, G. (2017). Repression of miR156 by miR159 regulates the timing of the juvenile-to-adult transition in *Arabidopsis*. *Plant Cell* **29**, 1293–1304. doi:10.1105/tpc.16.00975

- He, J., Xu, M., Willmann, M. R., McCormick, K., Hu, T., Yang, L., Starker, C. G., Voytas, D. F., Meyers, B. C. and Poethig, R. S. (2018). Threshold-dependent repression of *SPL* gene expression by miR156/miR157 controls vegetative phase change in *Arabidopsis thaliana*. *PLoS Genet.* **14**, e1007337. doi:10.1371/journal.pgen.1007337
- Helliwell, C. A., Chin-Atkins, A. N., Wilson, I. W., Chapple, R., Dennis, E. S. and Chaudhury, A. (2001). The *Arabidopsis* *AMP1* gene encodes a putative glutamate carboxypeptidase. *Plant Cell* **13**, 2115-2125. doi:10.1105/TPC.010146
- Huang, W., Pitorre, D., Poretska, O., Marizzi, C., Winter, N., Poppenberger, B. and Sieberer, T. (2015). *ALTERED MERISTEM PROGRAM1* suppresses ectopic stem cell niche formation in the shoot apical meristem in a largely cytokinin-independent manner. *Plant Physiol.* **167**, 1471-1486. doi:10.1104/pp.114.254623
- Huijser, P. and Schmid, M. (2011). The control of developmental phase transitions in plants. *Development* **138**, 4117-4129. doi:10.1242/dev.063511
- Leyser, H. M. O. and Furner, I. J. (1992). Characterization of three shoot apical meristem mutants of *Arabidopsis thaliana*. *Development* **116**, 397-403.
- Li, S., Liu, L., Zhuang, X., Yu, Y., Liu, X., Cui, X., Ji, L., Pan, Z., Cao, X., Mo, B. et al. (2013). MicroRNAs inhibit the translation of target mRNAs on the endoplasmic reticulum in *Arabidopsis*. *Cell* **153**, 562-574. doi:10.1016/j.cell.2013.04.005
- Li, J., Reichel, M. and Millar, A. A. (2014). Determinants beyond both complementarity and cleavage govern microR159 efficacy in *Arabidopsis*. *PLoS Genet.* **10**, e1004232. doi:10.1371/journal.pgen.1004232
- Millar, A. A. and Gubler, F. (2005). The *Arabidopsis* *GAMYB*-like genes, *MYB33* and *MYB65*, are microRNA-regulated genes that redundantly facilitate anther development. *Plant Cell* **17**, 705-721. doi:10.1105/tpc.104.027920
- Pesch, M., Schultheiß, I., Klopffleisch, K., Uhrig, J. F., Koegl, M., Clemen, C. S., Simon, R., Weidtkamp-Peters, S. and Hülskamp, M. (2015). TRANSPARENT TESTA *GLABRA1* and *GLABRA1* compete for binding to *GLABRA3* in *Arabidopsis*. *Plant Physiol.* **168**, 584-597. doi:10.1104/pp.15.00328
- Skopelitis, D. S., Hill, K., Klesen, S., Marco, C. F., von Born, P., Chitwood, D. H. and Timmermans, M. C. P. (2018). Gating of miRNA movement at defined cell-cell interfaces governs their impact as positional signals. *Nat. Commun.* **9**, 3107. doi:10.1038/s41467-018-05571-0
- Telfer, A., Bollman, K. M. and Poethig, R. S. (1997). Phase change and the regulation of trichome distribution in *Arabidopsis thaliana*. *Development* **124**, 645-654.
- Vidaurre, D. P., Ploense, S., Krogan, N. T. and Berleth, T. (2007). *AMP1* and *MP* antagonistically regulate embryo and meristem development in *Arabidopsis*. *Development* **134**, 2561-2567. doi:10.1242/dev.006759
- Wang, L., Zhou, C.-M., Mai, Y.-X., Li, L.-Z., Gao, J., Shang, G.-D., Lian, H., Han, L., Zhang, T.-Q., Tang, H.-B. et al. (2019). A spatiotemporally regulated transcriptional complex underlies heteroblastic development of leaf hairs in *Arabidopsis thaliana*. *EMBO J.* **38**, e100063. doi:10.15252/embj.2018100063
- Wu, G. and Poethig, R. S. (2006). Temporal regulation of shoot development in *Arabidopsis thaliana* by miR156 and its target *SPL3*. *Development* **133**, 3539-3547. doi:10.1242/dev.02521
- Wu, G., Park, M. Y., Conway, S. R., Wang, J.-W., Weigel, D. and Poethig, R. S. (2009). The sequential action of miR156 and miR172 regulates developmental timing in *Arabidopsis*. *Cell* **138**, 750-759. doi:10.1016/j.cell.2009.06.031
- Xu, M., Hu, T., Zhao, J., Park, M.-Y., Earley, K. W., Wu, G., Yang, L. and Poethig, R. S. (2016). Developmental functions of miR156-regulated *SQUAMOSA PROMOTER BINDING PROTEIN-LIKE (SPL)* genes in *Arabidopsis thaliana*. *PLoS Genet.* **12**, e1006263. doi:10.1371/journal.pgen.1006263
- Xu, Y., Qian, Z., Zhou, B. and Wu, G. (2019). Age-dependent heteroblastic development of leaf hairs in *Arabidopsis*. *New Phytol.* **224**, 741-748. doi:10.1111/nph.16054
- Yang, L., Conway, S. R. and Poethig, R. S. (2011). Vegetative phase change is mediated by a leaf-derived signal that represses the transcription of miR156. *Development* **138**, 245-249. doi:10.1242/dev.058578
- Yang, L., Wu, G. and Poethig, R. S. (2012). Mutations in the GW-repeat protein *SUO* reveal a developmental function for microRNA-mediated translational repression in *Arabidopsis*. *Proc. Natl. Acad. Sci. USA* **109**, 315-320. doi:10.1073/pnas.1114673109
- Yang, L., Xu, M., Koo, Y., He, J. and Poethig, R. S. (2013). Sugar promotes vegetative phase change in *Arabidopsis thaliana* by repressing the expression of *MIR156A* and *MIR156C*. *eLife* **2**, e00260. doi:10.7554/eLife.00260.017
- Yang, S., Poretska, O. and Sieberer, T. (2018). *ALTERED MERISTEM PROGRAM1* restricts shoot meristem proliferation and regeneration by limiting HD-ZIP III-mediated expression of *RAP2.6L*. *Plant Physiol.* **177**, 1580-1594. doi:10.1104/pp.18.00252
- Yu, S., Cao, L., Zhou, C.-M., Zhang, T.-Q., Lian, H., Sun, Y., Wu, J., Huang, J., Wang, G. and Wang, J.-W. (2013). Sugar is an endogenous cue for juvenile-to-adult phase transition in plants. *eLife* **2**, e00269. doi:10.7554/eLife.00269